Acta Crystallographica Section B
Structural Science
ISSN 0108-7681

1,1′-Fc(4-$C_6H_4CO_2Et)_2$ and its unusual salt derivative with *Z*′ = 5, *catena*-$[Na^+]_2$[1,1′-Fc(4-$C_6H_4CO_2^-)_2]\cdot 0.6H_2O$ [1,1′-Fc = (η^5-$(C_5H_4)_2Fe$]

John F. Gallagher,[a]* Steven Alley,[a] Marianne Brosnan[a] and Alan J. Lough[b]

[a]School of Chemical Sciences, Dublin City University, Dublin 9, Ireland, and [b]Department of Chemistry, 80 St George Street, University of Toronto, Toronto, Ontario, Canada M5S 3H6

Correspondence e-mail: john.gallagher@dcu.ie

Received 15 October 2009
Accepted 1 February 2010

The neutral diethyl 4,4′-(ferrocene-1,1′-diyl)dibenzoate, Fe[η^5-(C_5H_4)(4-$C_6H_4CO_2Et)]_2$ (I), yields (II) (following base hydrolysis) as the unusual complex salt poly[disodium bis[diethyl 4,4′-(ferrocene-1,1′-diyl)dibenzoate] 0.6-hydrate] or $[Na^+]_2$[Fe{η^5-(C_5H_4)-4-$C_6H_4CO_2^-\}_2]\cdot 0.6H_2O$ with *Z*′ = 5. Compound (I) crystallizes in the triclinic system, space group $P\bar{1}$, with two molecules having similar geometry in the asymmetric unit (*Z*′ = 2). The salt complex (II) crystallizes in the orthorhombic system, space group *Pbca*, with the asymmetric unit comprising poly[decasodium pentakis-[diethyl 4,4′-(ferrocene-1,1′-diyl)dibenzoate] trihydrate] or $[Na^+]_{10}$[Fe{η^5-(C_5H_4)-4-$C_6H_4CO_2^-\}_2]_5\cdot 3H_2O$. The five independent 1,1′-Fc[(4-$C_6H_4CO_2)^-]_2$ dianions stack in an offset ladder (stepped) arrangement with the ten benzoates mutually oriented *cisoid* towards and bonded to a central layer comprising the ten Na^+ ions and three water molecules [1,1′-Fc = η^5-$(C_5H_4)_2Fe$]. The five dianions differ in the *cisoid* orientations of their pendant benzoate groups, with four having their $-C_6H_4-$ groups mutually oriented at interplanar angles from 0.6 (3) to 3.2 (3)° (as $\pi\cdots\pi$ stacked C_6 rings) and interacting principally with Na^+ ions. The fifth dianion is distorted and opens up to an unprecedented $-C_6H_4-$ interplanar angle of 18.6 (3)° through bending of the two 4-$C_6H_4CO_2$ groups and with several ionic interactions involving the three water molecules (arranged as one-dimensional zigzag chains in the lattice). Overall packing comprises two-dimensional layers of Na^+ cations coordinated mainly by the carboxylate O atoms, and one-dimensional water chains. The non-polar $Fc(C_6H_4)_2$ groups are arranged perpendicular to the layers and mutually interlock through a series of efficient C—H$\cdots\pi$ stacking contacts in a herringbone fashion to produce an overall segregation of polar and non-polar entities.

1. Introduction

To date ferrocenyl derivatives have been the subject of intensive research in coordination chemistry given the important roles which the electroactive ferrocenyl core can provide in a diverse range of molecules and structures (Braga, Maini *et al.*, 2003; Braga, Polito *et al.*, 2003; Štěpnička, 2008; Štěpnička *et al.*, 2008). Its roles have encompassed both structural and electronic capabilities owing to the diversity of groups and their constituent donor atoms, *e.g.* N, O, P and S, that can be bonded directly to the ferrocenyl moiety (Štěpnička, 2008). Of interest amongst ferrocene derivatives are the dicarboxylic acid derivatives that have attracted considerable attention and the prime example studied thus far is ferrocene 1,1′-dicarboxylic acid [1,1′-Fc$(CO_2H)_2$] (III), where 1,1′-Fc =

η^5-$(C_5H_4)_2Fe$. Over 100+ structures containing the 1,1′-$Fc(CO_2)_2$ core are available on the Cambridge Structural Database (Allen, 2002; CSD version 5.30; four updates) and many of these systems are unusual supramolecular assemblies comprising two or more metals and with several ligands. The direct interaction of the ferrocenyl group in (III) with additional metal centres either through bridging and/or chelation modes is facilitated in supramolecular assemblies (refcode XUKFEO, Yang & Wong, 2002; refcode HOQSEL, Cotton *et al.*, 1999; refcode MOBHAM, Bera *et al.*, 2002; refcodes EDATUZ/EDAVAH/EDAVEL Masello *et al.*, 2007). In addition, (III) has been used extensively in hydrogen-bonding studies (Zakaria *et al.*, 2002, 2003; Braga *et al.*, 2000; Štěpnička, 2008).

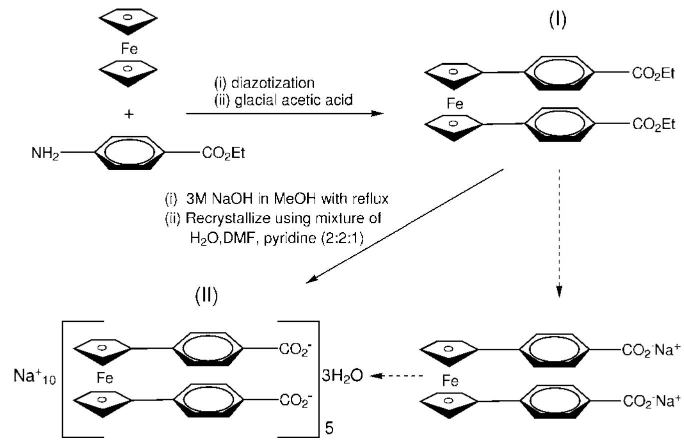

(I)

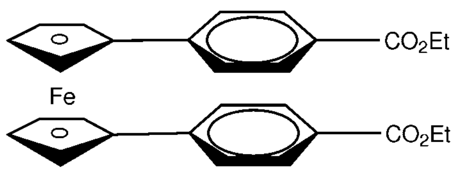

(II)

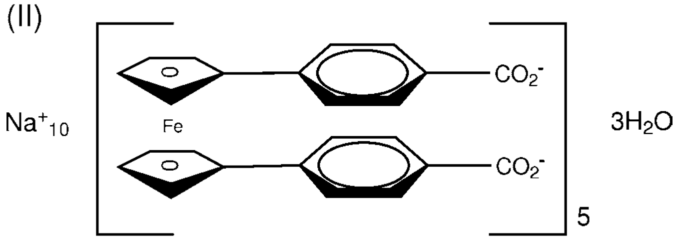

(III)

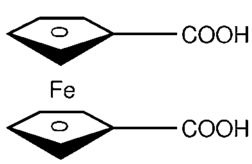

Herein we report the synthesis and structures of two new 1,1′-ferrocene systems (I) and (II), both derived from ferrocene and ethyl-4-aminobenzoate, with diagrams and tables as Schemes 1 and 2, Figs. 1–7 and Tables 1–5. The neutral 1,1′-bis{ethyl(4-benzoate)}ferrocene (I) or 1,1′-$Fc(4\text{-}C_6H_4CO_2Et)_2$, is synthesized in relatively low yield (see §2) and crystallizes in the triclinic system $P\bar{1}$ (No. 2) with two molecules similar in geometry ($Z' = 2$) in the asymmetric unit (Table 2). Molecule (I) is depicted in Figs. 1 and 2 with selected geometric data in Tables 2 and 3. Compound (I) yields a complex salt under base hydrolysis conditions with stoichiometry 1,1′-$Fc[(4\text{-}C_6H_4CO_2^-Na^+)_2]$ and crystallizes with difficulty over four weeks as small red crystals of $[Na^+]_2[\eta^5\text{-}(C_5H_4)_2Fe(4\text{-}C_6H_4CO_2^-)_2]\cdot 0.6H_2O$ (II).

2. Experimental

2.1. Synthesis and characterization

Synthesis of 1,1′-$Fc[4\text{-}C_6H_4CO_2C_2H_5]_2$ (I): the diazotization of ethyl 4-aminobenzoate (3.55 g, 22 mmol) was achieved by literature methods (Vogel *et al.*, 1996). The resulting solution was added to a cold ferrocene solution (2 g, 11 mmol) in glacial acetic acid (50 ml). The reaction mixture was allowed to warm to room temperature and stirred for 6 h: water was added and the resulting solution extracted with CH_2Cl_2 (3 ×

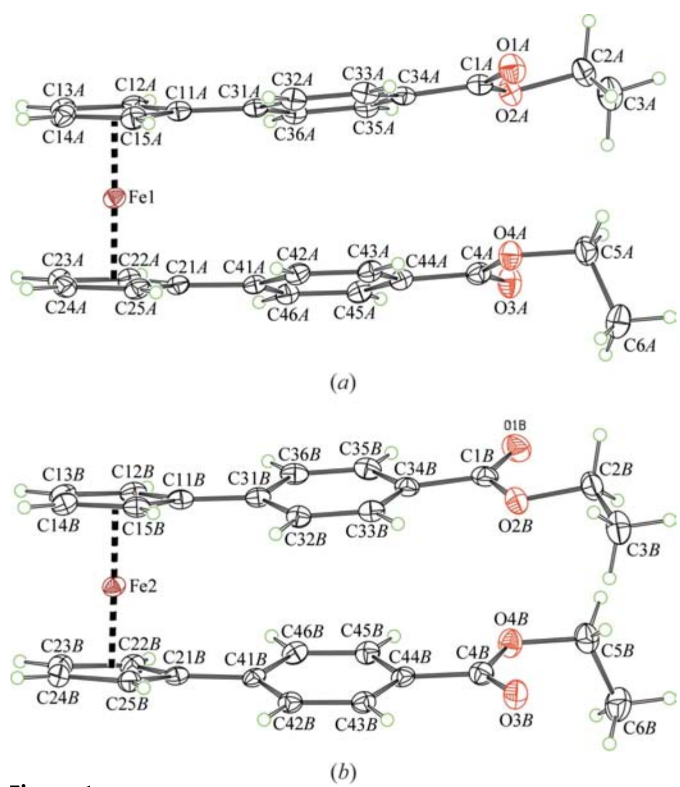

Figure 1
(*a*) A view of molecule *A* in (I) with atomic-numbering scheme. Displacement ellipsoids are drawn at the 30% probability level. (*b*) A view of molecule *B* in (I) with the atomic-numbering scheme. Displacement ellipsoids are depicted as above.

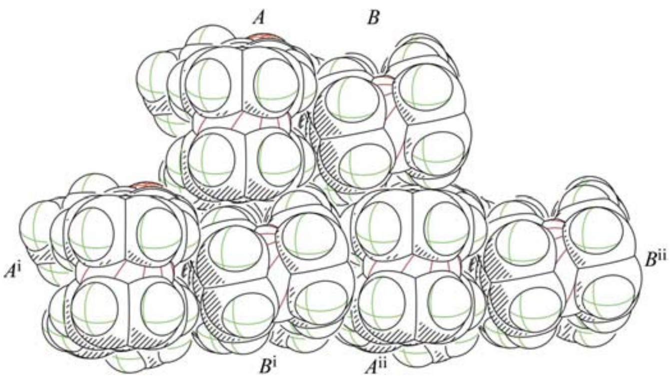

Figure 2
A view of the molecular stacking in the crystal structure of (I) with atoms drawn as their van der Waals spheres. Symmetry codes: (i) $1 + x, y, z$; (ii) $x, 1 + y, z$.

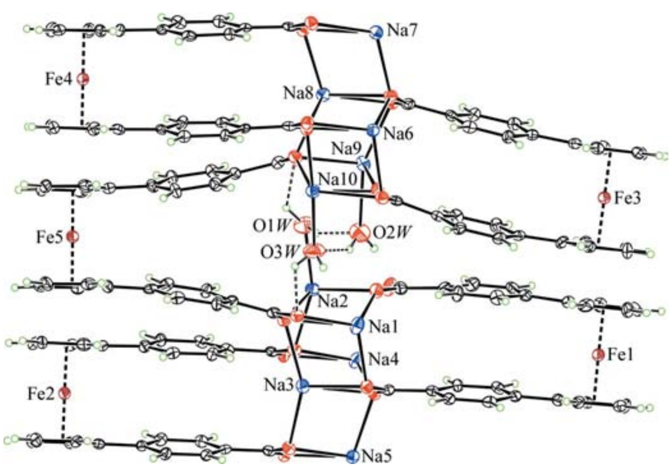

Figure 3
A view of the asymmetric unit in (II) with displacement ellipsoids depicted at the 30% probability level.

50 ml). The combined extracts were washed with 10% Na_2CO_3 (2×50 ml), H_2O (2×50 ml) and dried over $MgSO_4$. The solvent was removed and the resulting red oil purified by column chromatography using a solvent gradient of petroleum spirits to diethyl ether. The desired product eluted in 20% petroleum spirits:Et_2O and the solvent was removed to yield 0.18 g (3.5%) of 1,1′-Fc[4-$C_6H_4CO_2Et$]$_2$ as a red crystalline powder. M.p. 405–407 K. Anal.: calc for $C_{28}H_{26}O_4Fe$: C 69.72, H 5.43; found: C 69.36, H 5.40. UV λ_{max} nm, ε° (l mol^{-1} cm^{-1}): 457 (1160), 363 (3091), 301 (16908), 265 (22222). IR (KBr, cm^{-1}): 3103 (w), 2985 (w), 1713 (s, C═O), 1608 (m), 1419 (m), 1367 (w), 1277 (s), 1184 (m), 1110 (s), 851 (m), 815 (m), 772 (m), 698 (m). ^{1}H NMR ($CDCl_3$): δ 1.40 (3H, t, $^3J_{H-H}$ 7.2 Hz, CH_2CH_3), 4.34 (2H, s, H13), 4.37 (2H, q, $^3J_{H-H}$ 7.2 Hz, CH_2CH_3), 4.57 (2H, s, H12), 7.21 (2H, d, $^3J_{H-H}$ 7.6 Hz, H21/26), 7.81 (2H, d, $^3J_{H-H}$ 7.6 Hz, H23/25). ^{13}C NMR ($CDCl_3$): δ 14.36 ($CH_2\mathit{CH_3}$), 60.78 ($\mathit{CH_2}CH_3$), 68.61 (C12/15), 71.60 (C13/14), 85.23 (C11), 125.42 (C22/26), 127.75 (C24), 129.55 (C23/25), 142.95 (C21), 166.52 (C═O). ESMS (MeOH, CV 20 V): m/z 521 ([M+K$^+$]$^+$, 22%), 505 ([M+Na$^+$]$^+$, 100%), 482 ([M^+], 40%), 454 ([M^+−CH_2CH_3], 30%), 426 ([M^+-2CH_2CH_2]$^+$, 22%).

Synthesis of [Na$^+$]$_2$[Fc(4-$C_6H_4CO_2^-$])$_2$] (II): 1,1′-[Fc(4-$C_6H_4CO_2Et$)$_2$] (0.18 g, 0.4 mmol) was dissolved in 10 ml of methanol followed by the addition of 5 ml of 3M NaOH. The mixture was brought to reflux conditions and in 30 min the solution changed colour from red to orange and an orange precipitate fell from solution: after 2 h the solution was cooled and filtered. The filtrate was washed with cold water and dried to give 0.16 g (90%) of the 1,1′-Fc[4-$C_6H_4CO_2^-$Na$^+$]$_2$ salt as an orange powder. This product is sparingly soluble in polar organic solvents and water. Evaporation of a saturated solution of 1,1′-Fc[(4-$C_6H_4CO_2Na$)$_2$] in water/dimethylformamide/pyridine solution (2:2:1) over four weeks resulted in small red

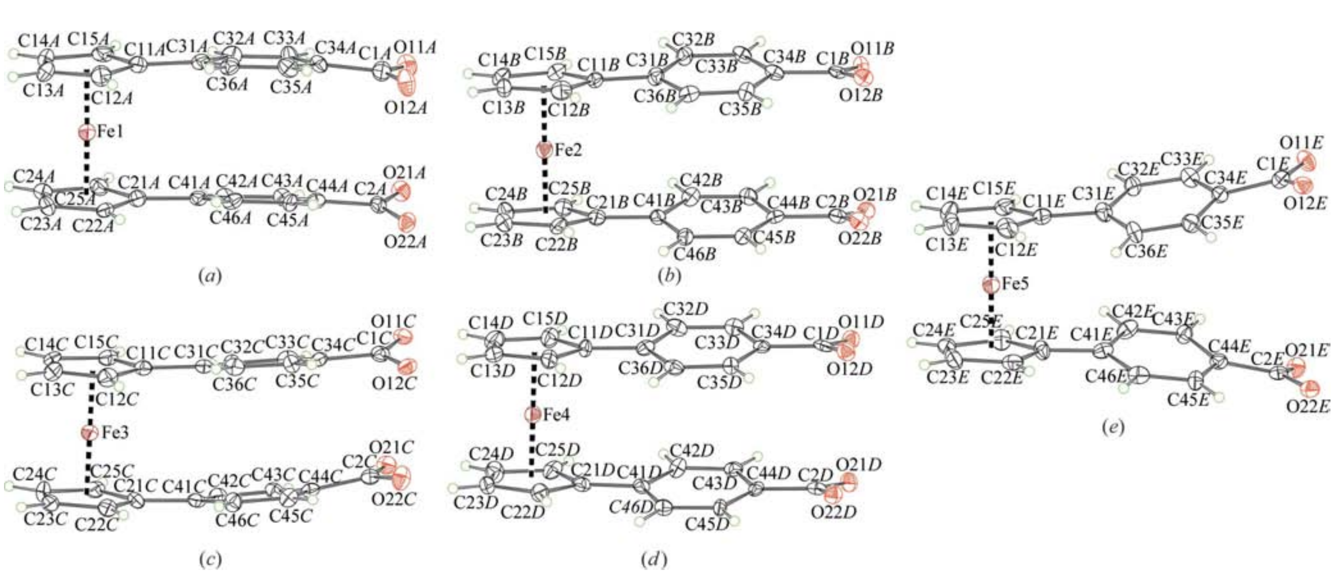

Figure 4
(*a*)–(*e*) Views of dianions *A*–*E* in (II) with atomic-numbering scheme. Displacement ellipsoids are drawn at the 30% probability level.

Table 1
Crystal data and experimental data collection parameters for (I) and (II).

Experiments were carried out at 150 K with Mo $K\alpha$ radiation using a Kappa-CCD diffractometer. Absorption was corrected for by multi-scan methods (*SORTAV*; Blessing, 1995).

	(I)	(II)
Crystal data		
Chemical formula	$C_{28}H_{26}FeO_4$	$C_{24}H_{16}FeNa_2O_4 \cdot 0.6H_2O$
M_r	482.34	2405.04
Crystal system, space group	Triclinic, $P\bar{1}$	Orthorhombic, *Pbca*
a, b, c (Å)	9.1028 (3), 9.6826 (5), 25.3805 (12)	36.4368 (10), 11.5998 (4), 45.8014 (11)
α, β, γ (°)	83.683 (2), 82.200 (3), 89.460 (3)	90, 90, 90
V (Å^3)	2202.82 (17)	19 358.4 (10)
Z	4	40
μ (mm^{-1})	0.72	0.86
Crystal size (mm)	0.30 × 0.26 × 0.24	0.15 × 0.10 × 0.05
Data collection		
T_{min}, T_{max}	0.638, 0.938	0.882, 0.958
No. of measured, independent and observed [$I > 2\sigma(I)$] reflections	19 022, 9803, 6524	31 468, 17 082, 6015
R_{int}	0.059	0.137
Refinement		
$R[F^2 > 2\sigma(F^2)]$, $wR(F^2)$, S	0.054, 0.142, 1.02	0.064, 0.158, 0.94
No. of reflections	9803	17 082
No. of parameters	599	1441
No. of restraints	0	9
H-atom treatment	H-atom parameters constrained	H atoms treated by a mixture of independent and constrained refinement
$\Delta\rho_{max}$, $\Delta\rho_{min}$ (e Å−3)	0.59, −0.81	0.59, −0.45

Computer programs used: *KappaCCD* Server Software (Nonius, 1997), *DENZO-SMN* (Otwinowski & Minor, 1997), *SHELXS*97 and *SHELXL*97 (Sheldrick, 2008), *PLATON* (Spek, 2009), *ORTEX* (McArdle, 1995), *PREP*8 (Ferguson, 1998).

Table 2
Selected torsion angle data in (I) (°).

C34*A*—C1*A*—O2*A*—C2*A*	171.4 (3)
C34*B*—C1*B*—O2*B*—C2*B*	−173.8 (3)
C4*A*—O4*A*—C5*A*—C6*A*	−87.8 (4)
C4*B*—O4*B*—C5*B*—C6*B*	85.7 (4)
C12*A*—C11*A*—C31*A*—C36*A*	−12.6 (4)
C12*B*—C11*B*—C31*B*—C32*B*	−168.8 (3)
Fe1—C11*A*—C31*A*—C36*A*	78.6 (3)
Fe2—C11*B*—C31*B*—C32*B*	−78.0 (4)

crystals of (II) suitable for analysis by X-ray diffraction. ESMS (MeOH/H_2O, CV −20 V): m/z 426 $(M-H^+)^-$, 100%.

2.2. Crystal structure determination, refinement and computing details

Molecule (I) crystallized in the triclinic system: space group $P\bar{1}$ (No. 2) assumed and confirmed by the analysis. Molecules *A* and *B* were chosen within the unit cell in proximity to the origin in order to maximize hydrogen bonding and contacts between the pair (within the asymmetric unit): choosing either an inverted *A* or *B* molecule positions this molecule at a much greater distance from its partner: see refinement details in Table 1 and the supplementary materials.[1] The complex salt (II) crystallized in the orthorhombic system: space group *Pbca* (No. 60) from the systematic absences. The structure of $[Na^+]_2[\eta^5\text{-}(C_5H_4)_2Fe(4\text{-}C_6H_4\text{-}CO_2^-])_2]\cdot 0.6H_2O$ was solved by a direct methods program (*SHELXS*97, Sheldrick, 2008) without particular difficulty.

All H atoms bound to C were treated as riding atoms with the *SHELXL*97 defaults at 150 K (Sheldrick, 2008) for C—H distances 0.99 Å CH_2, 0.98 Å CH_3 and 0.95 Å [for aromatic and η^5-(C_5H_4)] and with $U_{iso}(H) = 1.5U_{eq}(C)$ for methyl H atoms and $1.2U_{eq}(C)$ for the remainder (CH_2 and aromatic C—H). In (II) the nine restraints comprise six 'soft' *DFIX* restraints on the O—H bond length and three H···H restraints on the H—O—H angle.

[1] Supplementary data for this paper are available from the IUCr electronic archives (Reference: BK5092). Services for accessing these data are described at the back of the journal.

3. Results and discussion

3.1. Molecular and crystal structure of (I)

In (I) the Fe—C bond lengths involving the four η^5-(C_5H_4) rings in molecules *A* and *B* lie within expected ranges (Table 3). The four longest Fe—C distances involve the *ipso*-C(1/2)1[*A*/*B*] from 2.067 (3) to 2.072 (3) Å and the remaining 16 Fe—C distances span a narrow range from 2.035 (3) to 2.052 (3) Å. The substituted η^5-(C_5H_4) rings are essentially eclipsed with C1*mn*···*Cg*···*Cg*···C2*mn* (m = 1–5, $n = A, B$) torsion angles in the range −3.8 (2) to −4.3 (2)° in *A* and 2.6 (2) to 3.1 (2)° *B* (Table 3). The essentially parallel η^5-$(C_5H_4)_2$Fe rings have centroids (Cg) separated by 3.2974 (19) and 3.3027 (19) Å: the almost parallel —C_6H_4— rings have ring centroids 3.4949 (17) (*A*) and 3.5059 (17) Å (*B*) apart (the shortest C···C interplanar distances are 3.31 and 3.33 Å, respectively). Both molecules *A* and *B* are similar and geometric data (Tables 2 and 3) correspond with the mono-substituted methyl, ethyl and isopropyl 4-ferrocenylbenzoates (Savage *et al.*, 2002; Anderson *et al.*, 2003), although differing from the dianions in (II). A subtle feature in (I) is the slight bending along the 4-(C_5H_4)$C_6H_4CO_2$ groups with the four *ipso*-C(1/2)1[*A*/*B*] cyclopentadienyl atoms removed by 0.047 (4) to 0.084 (4) Å from their respective attached C_6 planes and in the same direction as the C(1/4)[*A*/*B*] carboxylate atoms [by 0.080 (5) to 0.092 (5) Å]. Within the C_6 rings the eight substituted atoms C(3/4)[1/4]{*A*/*B*} distort slightly from planarity towards a 1,4-boat conformation by 0.004 (2) to 0.015 (2) Å (from the C_6 mean plane). Molecules *A* and *B* aggregate in pairs and are chosen so that the inverted

Table 3
Selected bond lengths and angles in (I) (Å, °).

Bond/angle (Å, °)	Molecule *A*	Molecule *B*
Fe···*Cg*†	1.6491 (15)/1.6485 (13)	1.6526 (15)/1.6501 (14)
Fe—C range	2.035 (3)–2.068 (3)	2.035 (3)–2.072 (3)
$Fe—C_{cp}—C_{ar}$	125.8 (2)/128.5 (2)	125.9 (2)/128.6 (2)
Cg···Fe···*Cg*†	179.40 (7)	179.22 (8)
C1*mn*···*Cg*···*Cg*···C2*mn*†‡	−4.0 (2)	2.8 (2)
C_5H_4/C_5H_4	2.0 (2)	1.9 (2)
C_6/C_6	3.55 (17)	4.12 (17)
C═O	1.209 (4)/1.210 (4)	1.212 (4)/1.213 (4)
C—O	1.347 (4)/1.344 (4)	1.343 (4)/1.340 (4)
O═C—O	122.9 (3)/123.5 (3)	123.4 (3)/123.5 (3)

† *Cg* represents ring centroids as *Cg*1/*Cg*2 and *Cg*3/*Cg*4 in the C_5H_4 rings. ‡ Average data for C1*mn*···*Cg*···*Cg*···C2*mn* torsion angles (*m* = 1–5: *n* = *A*,*B*).

B (as *B**) and *A* have a close fit with differences for the weighted and unit-weight r.m.s. fit of 0.065 and 0.052 Å. There are no classical hydrogen bonds in the crystal structure of (I) and only weak C—H···O interactions are present.

The number of 1,1′-Fc$[C_6]_2$ structures is small in comparison to derivatives of (III), and both *cisoid* and *transoid* geometries are known. An example of a *cisoid* conformation is the structure of XEQJUY or 1,4-bis(1′-pentafluorophenyl)ferrocenyl-2,3,5,6-tetrafluorobenzene (Deck *et al.*, 2000) and a *transoid* conformation is observed in 1,1′-bis(4-(4-pyridyl)phenyl)ferrocene (BATFIM; Braga, Polito *et al.*, 2003). In 1,1′-bis(9-anthracenyl)ferrocene (NOHGUM), the two substituted C_5H_4 rings though eclipsed have their *ipso*-C atoms staggered by *ca* 72° with the 9-anthracenyl rings oriented with an interplanar angle of 56.18 (12)°: steric effects from flanking anthracenyl C—H groups force a twist above and below the substituted cyclopentadienyl ring planes (Butler *et al.*, 1997).

3.2. Molecular and crystal structure of (II)

Crystals of (II) were obtained with difficulty due to solubility problems encountered when using the 1,1′-Fc[(4-$C_6H_4CO_2Na)_2$] salt and many attempts were made to procure a suitable solvent system to induce crystallization. Over a protracted period of time the starting material was recrystallized from a range of solution mixtures and typically yielded microcrystalline powders. Suitable crystals for diffraction were finally isolated from a 2:2:1 solution of water/dimethylformamide/pyridine left over a 4 week period to yield the complex salt (II) determined by structural analysis as $[Na^+]_2[\eta^5\text{-}(C_5H_4)_2Fe(4\text{-}C_6H_4CO_2^-)_2]\cdot 0.6H_2O$, with Z' = 5.

The five dianions *A*–*E* are depicted in Figs. 4(*a*)–(*e*) with the asymmetric unit as Fig. 3 and local hydrogen bonding and packing arrangements in Figs. 5–7. Tables of important geometric data such as torsion angles, interplanar and hydrogen bonding data are provided in Tables 4 and 5. The bond lengths and angles are typical of ferrocene derivatives as for (I) and (III), but the torsion and plane angle data exhibit

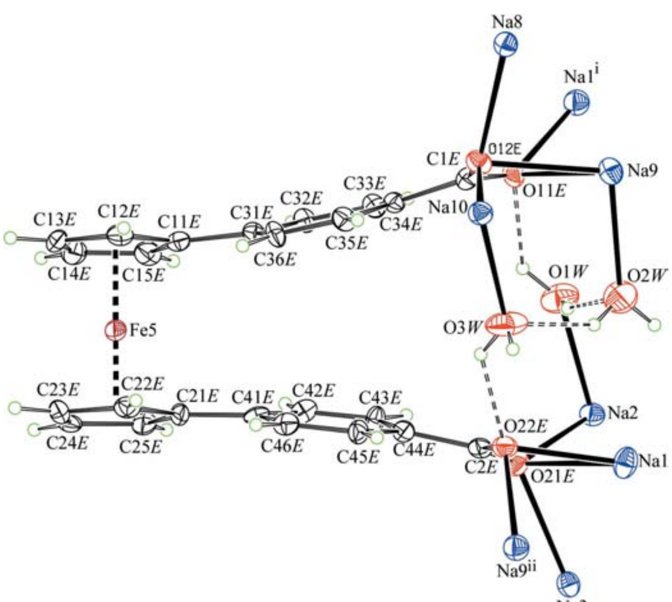

Figure 5
A view of dianion *E* with the three water molecules O1*W*, O2*W*, O3*W* and six Na cations Na1–3, Na8–10 that are involved in the coordination sphere. Displacement ellipsoids are depicted at the 30% probability level. The symmetry operations are (i) $1-x, \frac{1}{2}+y, \frac{1}{2}-z$ and (ii) $1-x, -\frac{1}{2}+y, \frac{1}{2}-z$.

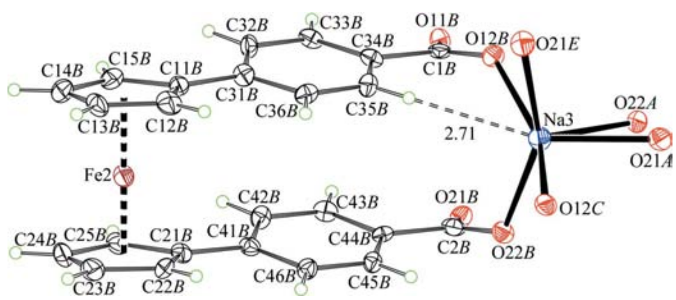

Figure 6
A view of dianion *B* with the C—H···Na3 contact in (Å). The distorted six-coordination is shown for Na3 and displacement ellipsoids are depicted at the 30% probability level.

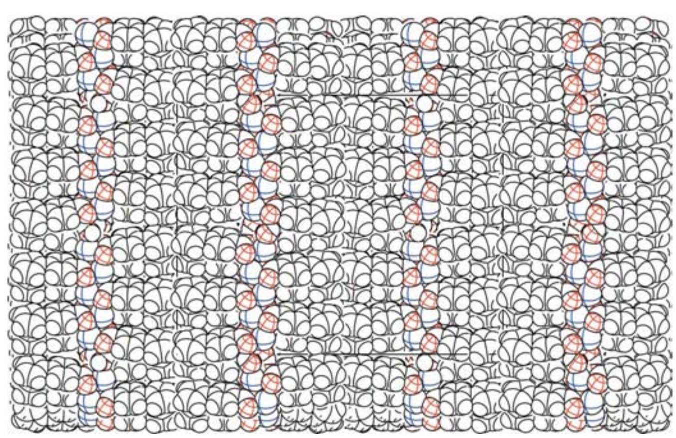

Figure 7
An extended view along the [010] direction showing the extended sheets comprising the one-dimensional chain of water molecules and columns of Na^+ ions and carboxylates sandwiched between the non-polar 1,1-$Fc(C_6H_4)_2$ groups.

Table 4
Comparison of selected bond lengths, angles (Å, °) in the five dianions of (II).

Bond/angle (Å, °)	*A*	*B*	*C*	*D*	*E*
Ferrocenyl group†‡§					
Fe—C minimum	2.025 (6)	2.031 (7)	2.026 (6)	2.026 (6)	2.023 (6)
Fe—C maximum	2.066 (6)	2.076 (6)	2.084 (6)	2.079 (6)	2.061 (7)
$Fe_n\cdots Cg$	1.651 (3)	1.660 (3)	1.657 (3)	1.654 (3)	1.644 (3)
$Fe_n\cdots Cg$	1.645 (3)	1.646 (3)	1.650 (3)	1.656 (3)	1.644 (3)
$Cg\cdots Fe_n\cdots Cg$	178.56 (17)	179.49 (16)	179.12 (17)	179.34 (17)	179.27 (17)
C1*mn*···*Cg*···*Cg*···C2*mn*	−4.2 (5)	4.5 (5)	−6.1 (5)	5.9 (5)	−4.4 (4)
C1*mn*···*Cg*···*Cg*···C2*mn*	−5.3 (5)	5.8 (5)	−7.4 (5)	7.4 (5)	−5.9 (4)
C1*n*···C11*n*···C21*n*···C2*n*	−5.59 (15)	5.62 (15)	−7.35 (15)	6.51 (14)	−9.62 (19)
Fe—C11*n*—C31n_{ar}§	128.8 (4)	128.7 (4)	130.0 (4)	128.4 (4)	130.2 (5)
Fe—C21*n*—C41n_{ar}§	127.1 (4)	126.5 (4)	125.3 (4)	125.2 (4)	128.7 (5)
Carboxylate CO_2^-,¶ C_6					
C1*n*—O11*n*/C1*n*—O12*n*	1.261 (8)	1.265 (7)	1.266 (7)	1.264 (7)	1.265 (7)
O11*n*—C1*n*—O12*n*	123.4 (6)	123.8 (6)	122.7 (6)	123.3 (6)	123.8 (6)
C2*n*—O21*n*/C2*n*—O22*n*	1.270 (7)	1.259 (7)	1.262 (7)	1.259 (7)	1.263 (7)
O21*n*—C2*n*—O22*n*	122.0 (6)	123.3 (6)	123.6 (6)	123.2 (6)	122.5 (6)
C31*n*···C41*n*	3.432 (9)	3.387 (9)	3.448 (10)	3.391 (9)	3.460 (9)
C34*n*···C44*n*	3.541 (9)	3.456 (9)	3.484 (9)	3.465 (9)	4.331 (9)
C1*n*···C2*n*	3.530 (10)	3.448 (9)	3.400 (9)	3.463 (9)	5.113 (9)
C1*n*···Fe···C2*n*	28.33 (8)	27.62 (7)	27.22 (7)	27.76 (7)	40.59 (7)
C1*n*···C31*n*···C11*n*	174.6 (4)	178.1 (5)	177.2 (4)	179.7 (5)	172.3 (4)
C2*n*···C41*n*···C21*n*	177.8 (4)	179.3 (5)	172.0 (4)	178.2 (4)	172.2 (4)
Interplanar angles					
C_5H_4/C_5H_4	1.6 (5)	0.3 (5)	1.5 (5)	1.2 (5)	0.7 (5)
C_5H_4/C_6H_4	7.3 (4)	11.1 (4)	11.2 (4)	10.6 (4)	17.4 (4)
C_5H_4/C_6H_4	11.2 (4)	12.4 (4)	10.2 (4)	10.1 (4)	16.0 (4)
C_6H_4/C_6H_4	3.2 (3)	1.3 (3)	2.1 (3)	0.6 (3)	18.6 (3)

† *Cg* is the C_5H_4 ring centroid for {C11*n*, …, C15*n*}, {C21*n*, …, C25*n*}: (*n* = *A*–*E*). ‡ Average values for the C1*mn*···*Cg*···*Cg*···C2*mn* torsion angles (*m* = 1–5; *n* = *A*–*E*). § The two Fe—C_{cp}—C_{ar} angles per dianion. ¶ Average of the two C—O distances for every CO_2^- moiety (*n* = *A*–*E*).

Table 5
Hydrogen-bond geometry in (II) (Å, °).

D—H···*A*	*D*—H	H···*A*	*D*···*A*	*D*—H···*A*
O1*W*—H12···O11*E*	0.91 (5)	2.16 (6)	2.793 (6)	126 (6)
O1*W*—H11···O2*W*	0.90 (5)	2.01 (4)	2.837 (9)	153 (8)
O2*W*—H22···O11*A*	0.90 (5)	2.04 (4)	2.849 (6)	150 (7)
O2*W*—H21···O3*W*	0.90 (5)	2.14 (4)	2.906 (9)	143 (6)
O3*W*—H32···O22*E*	0.91 (6)	2.02 (6)	2.714 (6)	132 (7)
O3*W*—H31···O1W^{i}	0.90 (5)	1.98 (4)	2.772 (8)	146 (7)

Symmetry codes: (i) $-x+1, y-\frac{1}{2}, -z+\frac{1}{2}$.

significant differences between the five dianions and typical ferrocene systems.

3.2.1. Supramolecular structure of (II). The outstanding feature of (II) is the structure of the complex salt $[Na^+]_2[\eta^5\text{-}(C_5H_4)_2Fe(4\text{-}C_6H_4CO_2^-)_2]\cdot 0.6H_2O$ with $Z' = 5$, isolated as the only crystalline product instead of the expected 1,1′-Fc[(4-$C_6H_4CO_2^-Na^+$)$_2$] derivative. The gross structural details are as follows: an aggregate set of five Fc[(benzenecarboxylate)$_2$]$^{2-}$ moieties crystallize in the asymmetric unit and stack in an offset step-ladder arrangement whereby the ten benzene carboxylates are oriented *cisoid* and bonded to a central plane comprising the ten Na^+ cations and with three hydrogen-bonding water molecules filling a void between the central distorted Fc[(benzenecarboxylate)$_2$]$^{2-}$ (*E*) and two flanking dianions (*A* and *C*; see Figs. 3 and 5). The water molecules O1*W*–O3*W* are linked to form one-dimensional zigzag chains in the crystal structure along the [010] direction with chains situated at the positions (0/0.5, *y*, 0.25/0.75) and with four chains per unit cell. In between these chains of water molecules lie columns of Na^+ cations as depicted in Fig. 7 (to highlight the combined effect of the one-dimensional $(H_2O)_n$ chains and Na^+ columns generating the cationic/H_2O two-dimensional sheets). These sheets combining Na^+ cations with H_2O chains are effectively sandwiched between the stacked dianions (between a 'wall' of dianion carboxylate O atoms) and are located at (*x*, *y*, 0.25/0.75) and parallel to (001) (Fig. 7). Each of the Na^+ ions is effectively surrounded by six O atoms (from carboxylate and water O atoms) and the shortest $Na^+\cdots Na^+$ distance is 3.146 (4) Å.

The effect of the sheet comprising Na^+ ion columns and chains of water molecules is to create a distinct boundary in the crystal structure where the cationic sheets and those parallel to (001) interact with a wall of anionic carboxylates from the stacked dianions. This arrangement of ions in the complex salt (II) is unusual and contains several interesting features as discussed below.

3.2.2. Molecular features of (II) – gross details. The five dianions *A* to *E* are distinctly different and close scrutiny reveals that four (*A* to *D*) have similar geometries with small differences in their C_6/C_6 interplanar angles [0.6 (3)–3.2 (3)°; Figs. 4*a*–*d*], but the fifth dianion (*E*) differs with its C_5H_4—$C_6H_4CO_2$ groups opened up and bent to an unexpected 18.6 (3)° (Fig. 4*e*, Table 4). The distortion in *E* arises from the formation and stability of $CO_2^-\cdots Na^+$ ionic bonds with additional hydrogen-bonding interactions. It is pertinent to distinguish between twisting (about C—C axes) and bending along the pendant C_5H_4—$C_6H_4CO_2$ groups: Fig. 4(*e*) highlights the deformation in *E*. The bending is demonstrated by the carboxylate C1*E* atom located 0.93 (2) Å from the η^5-C_5H_4 [C11*E*/C12*E*/C13*E*/C14*E*/C15*E*] plane and in the opposite direction to Fe5, whereas the carboxylate C2*E* atom is 0.78 (2) Å from its respective [C21*E*/C22*E*/C23*E*/C24*E*/C25*E*] C_5 plane and with a C1*E*···C2*E* separation of 5.113 (9) Å. This distance emphasizes the opening up of the C_6—CO_2 groups of dianion *E* in contrast to a simple rotation about either the aromatic C—C or Cg···Fe···Cg axes (Fig. 4*e*). In dianions *A*, *B* and *D*, the analogous bending distortions are such that the $C_{carboxylate}$ to C_5H_4 plane distances are < 0.30 Å and the dianions are relatively unperturbed in their respective environments (Figs. 4*a*, *b* and *d*), with C1*n*···C2*n* distances from 3.448 (9) to 3.530 (10) Å. However, in dianion *C* the deformation is such that the two pendant $-C_6H_4CO_2$ groups are bent in the same direction with the carboxylate C1*C*, C2*C* atoms displaced by 0.54 (2), 0.70 (2) Å from their respective C_5H_4 planes (Fig. 4*c*), with the carboxylate C1*A*···C2*C* distance contracting to 3.400 (9) Å. This deformation is unusual but not as dramatic as in *E* and can be explained by the unusual local environments of the carboxylates in *C*. Bending is also significant within the C_6 aromatic rings and for dianion *E* the two C31*E*/C34*E* atoms are displaced from the mean C_6 aromatic plane by 0.028 (5)/0.030 (5) Å and in the opposite direction to the four C32*E*/C33*E*/C35*E*/C36*E* atoms [displaced slightly by 0.010 (5) to 0.019 (5) Å towards a 1,4-boat]. For the C41*E*/C44*E* atoms, the data are 0.020 (5)/0.024 (5) Å and opposite C42*E*/C43*E*/C45*E*/C46*E* [0.007 (5) to 0.015 (4) Å]. Of the remaining eight C_6 groups only the C41*C*/C44*C* atom pair show similar distortions from C_6 planarity and by 0.026 (5)/0.029 (5) Å.

3.2.3. Molecular features of (II) – ferrocene details. The ferrocene moieties are relatively unperturbed in the five dianions (although some trends arise) as shown by:

(i) The range of $Fe-C_{cp}$ bond lengths (cp = C_5H_4) is typical for ferrocene derivatives from 2.023 (6) to 2.084 (6) Å, with the longest $Fe-C_{cp}$ bonds involving the substituted C atoms as the Fe—C11*n*/C21*n* bond (*n* = *A*–*E*) [for C11*n* the range is 2.066 (6) to 2.084 (6) Å; Table 4].

(ii) The range of Fe···*Cg* distances is normal and from 1.644 (3) to 1.660 (3) Å, with all *Cg*···Fe···*Cg* angles > 178.5° and cp/cp interplanar angles essentially parallel (< 2°).

(iii) Both pendant $-C_6H_4-CO_2^-$ groups are almost eclipsed with C1*mn*···*Cg*···*Cg*···C2*mn* angles in the range 3.2 (5)–7.4 (5)° (in absolute terms) for all five dianions (Table 4): using the carboxylate C1*n*/C2*n* atoms in calculations this range is 5.59 (15)–9.62 (19)°. These rotation angles are small and do not greatly influence the bending in dianions *C* and *E*. However, the molecular distortion is discernible from the $Fe-C_{cp}-C_{ar}$ bond angles of 125.2 (4)° (Fe4—C21*D*—C41*D*) to 130.2 (5)° (Fe5—C11*E*—C31*E*), with the two Fe—C—C angles > 130° present in dianions *C* and *E*.

(iv) The C_5H_4/C_6H_4 interplanar angles show a slight twisting of *ca* 10° [7.3 (4)–12.4 (4)°] between the C_5/C_6 planes in *A*–*D* and increasing to 17.4 (4)/16.0 (4)° in *E*. However, the parallel C_6H_4 interplanar angles of 0.6 (3)° (*D*) to 3.2 (3)° (*A*) contrasts with the C_6/C_6 interplanar angle of 18.6 (3)° in *E*. Together with the additional deformation data the differences are clearly distinct in *A*–*D* in comparison with dianion *E* (Table 4).

For comparisons with (II), a CSD search was analysed for $[C_5H_4-C]_2Fe$ compounds with no errors, disorder and with $R < 0.10$ to give a total of 684 'hits' and 894 observations (CSD version November 2008 and four updates). The average $Fe-C_{cp}$ bond length is 2.05 (1) Å and $Fe-C_{cp}-C_{external}$ angle is 125.5 (2)° (this average data has the $C_{external}$ as all 'types' and only using the C_{cp} atom substituted by the $C_{external}$ atom). In (II) the corresponding substituted $Fe-C_{cp}$ bond lengths are 0.03 Å longer with $Fe-C_{cp}-C_{ar}$ angles 3–5° larger (Table 4) than the CSD average values (regardless of the criteria used for $C_{external}$). For a restricted analysis with the external 'C' atom changed to '3' coordination (for 340 'hits'/435 observations) a Fe—C bond length of 2.04 (1) Å and Fe—C—C of 124.5 (3)° is noted: including a cyclic parameter on $C_{external}$ gives 2.05 (1) Å, 125.3 (3)° (113 'hits'/155 observations).

3.2.4. Molecular features of (II) – benzene carboxylate details. Deformations of the pendant $-C_6H_4-CO_2^-$ are evident from analysis of the trend of C···C distances for C31*n*···C41*n*, C34*n*···C44*n* and C1*n*···C2*n*. The carboxylate C1*n*···C2*n* (*n* = *A*–*D*) separations are 3.400 (9)–3.530 (10) Å for dianions *A*–*D*, but increasing to 5.113 (9) Å in dianion *E* (Table 4). In *A*, *B* and *D* the distances increase from C31*n*···C41*n* to C34*n*···C44*n*, C1*n*···C2*n*: however, *C* differs (with pendant groups bent in the same direction), and for *E* the C···C separation increases from C31*E*···C41*E* [3.460 (9) Å], C34*E*···C44*E* [4.331 (9) Å] to C1*E*···C2*E* [5.113 (9) Å]. Data for dianions *C* and *E* are rationalized as deformation of the pendant arms in the same direction in *C* and opposite direction (or opening up) in *E*.

The C1*n*—Fe—C2*n* angles also emphasize bending and 27.22 (7)° in *C* to 28.33 (8)° in *A* and contrasting with 40.59 (7)° in *E* (C1*E*···Fe5···C2*E*). Group distortion arises in the carboxylate C1*n*···C31*n*—C11*n* and C2*n*···C41*n*—C21*n* angles which are almost linear and > 175°, but in *E* distort to 172.2 (4) and 172.3 (2)°. Within the carboxylate moieties, delocalization is as expected (Table 4).

3.2.5. The coordination environment of the ten Na^+ ions. The coordination environment for all ten Na^+ ions shows a high degree of similarity both in terms of the coordination environment and bond length/angle data. The ten Na^+ ions form columns and with the three water molecules (as one-dimensional chains) combine to generate two-dimensional sheets in the lattice of (II). These two-dimensional sheets are effectively sandwiched between walls of interweaving carboxylate O atoms from the five dianions, forming a layer of width *ca* 6 Å (Figs. 3 and 7).

Eight of the ten Na^+ ions are coordinated by six O atoms using the ten carboxylates and three water molecules with Na^+···O distances from 2.201 (5) to 2.815 (5) Å: the Δ range (Å) for the six Na^+···O distances is < 0.50 Å for the eight Na^+ ions. The remaining Na1 and Na4 cations are coordinated by five short Na^+···O bonds plus one longer Na^+···O interaction at 3.131 (6) Å (Na1) and 2.979 (5) Å (Na4). The sixfold coordination at each Na^+ is accommodated *via* a $[CO_2^-Na^+]$ chelate involving two O atoms with the four remaining Na^+···O bonds involving either $Na^+\cdots O_{carboxylate}$ or a combination of $Na^+\cdots O_{carboxylate}$ and $Na^+\cdots O_{water}$ bonding. The three water molecules provide a balance in the mismatch between the number of Na^+ ions and carboxylate oxygen donors. The coordination geometry of the Na^+ ions deviates from standard six-coordinate and can be described as a distorted trigonal prism, with the two chelating carboxylate O atoms defining a prism side as for Na3 in Fig. 6. The Na^+ ions are offset from the centroids of the six O atoms. An alternative interpretation as a distortion from square-pyramidal geometry with the two CO_2 group O atoms occupying 'one' vertex and the remaining four O atoms in the basal plane has validity for Na1 and Na4 (see above). Of interest is that 16 of the 20 carboxylate O atoms form an ionic bond with three Na^+ ions, except for O11*A*, O11*E*, O22*C* and O22*E* which form only two O···Na^+ ionic bonds, but these four O atoms form some of the shortest Na^+···O ionic bonds due to the increased ionic bonding character over two Na^+···O bonds and also influenced by neighbouring water molecules. The shortest C—H···Na^+ contact involves Na3 (2.71 Å; Fig. 6) and the Na^+ ions are not involved in any other significant interaction.

Analysis of potential Na^+···Na^+ contacts shows Na1···Na9[i] [symmetry operation (i) = $1-x, -\frac{1}{2}+y, \frac{1}{2}-z$] to be the shortest at 3.146 (4) Å. From CSD analyses on Na···Na contacts, such Na···Na distances in metal-organic crystal structures are rarely < 3 Å. For the 33 structures (analysed as Na···O···Na on the CSD) the systems are typically air-sensitive materials with a bridging O atom containing μ_3-^{t}BuO or siloxy variants thereof, as in the europium compound with Na···Na distances of 2.92–2.94 Å, Na_8^+[(μ_4-*tert*-butoxo)-octakis(μ_3-*tert*-butoxo)-*tert*-butoxy-(μ_9-Cl)Eu] (WALRUW; Evans *et al.*, 1993). Carboxylate derivatives do not feature in structures with short Na^+···Na^+ distances, presumably due an increased tendency of carboxylates to chelate or semi-chelate these alkali metal ions.

In *catena*-[(μ_4-bis(4-methoxycarbonylbenzenesulfonyl)-amide)(μ-aqua)sodium] (GUNRUC) and two related K^+ structures (Moers *et al.*, 2001*a*) the organic layers are bonded to inorganic layers *via* alkali-metal$^+$···O ionic bonds and are similar to the layers described in (II). In GUNRUC bending of 6–7° occurs in the aromatic rings to compensate for the demands of ionic bonding. The coordination at the Na^+ ion is distorted octahedral with three *trans* O—Na—O angles from 168.10 (7) to 170.63 (7)° and a narrow range of six Na—O distances from 2.303 (2) to 2.4614 (19) Å. The $M^+N[SO_2C_6H_4$-4-$CO_2H]_2$, M^+ = K^+, Rb^+, Cs^+ structures (Moers *et al.*, 2001*b*) can also be classified as organic inorganic solids with self-assembly of parallel layers occurring through exhaustive hydrogen bonding: the structures are similar to GUNRUC (Moers *et al.*, 2001*a*) and (II) in layer formation. The three XAMWOX/XAMWUD/XAMXAK structures (Moers *et al.*, 2000) are comparable, although with smaller organic components. In broad terms, although the molecular and crystal structure of (II) is unique, there are several structures on the CSD which are related in terms of cation/anion binding and layer formation.

3.2.6. Hydrogen bonding and interactions in (II). Given the intricate molecular and crystal structure of (II), the overall hydrogen-bonding scheme, however, is uncomplicated. There are six O—H···O hydrogen bonds involving the three water molecules and three of these interactions are used to form a one-dimensional zigzag chain along the [010] direction as [O1*W*—H11···O2*W*—H21···O3*W*—H31···O1*W*^{i}]$_n$ (Fig. 3, Table 5). The three remaining O—H···O hydrogen bonds involve carboxylate O atoms O11*A*, O11*E* and O22*E* as $_{water}$O—H···O$_{carboxylate}$ within the asymmetric unit. Therefore, only one interaction as O3*W*···O1*W*^{i} links the one-dimensional chains of water molecules between asymmetric units along the [010] direction: the symmetry operation (i) $1-x, -\frac{1}{2}+y, \frac{1}{2}-z$ (Figs. 3 and 5, Table 5). In addition, there are three relatively short C—H···π(arene) interactions with C—H···Cg angles in the range 135–140° and with C···Cg distances from 3.403 (7) to 3.499 (7) Å. There are weak C—H···Na^+ contacts as depicted for Na3 (Fig. 6): this is a destabilizing contact and there are only two other similar H···Na^+ < 2.9 Å with a relatively minor impact on the structure of (II).

3.3. Summary of the overall structure of (II)

The structure of (II) is unusual, not least in that a complex salt crystallizes from solution as $[Na^+]_2$[1,1-Fc(4-$C_6H_4CO_2^-)_2]\cdot0.6H_2O$ and with Z' = 5 (Fig. 3) instead of the expected ferrocenyl salt 1,1′′-Fc(4-$C_6H_4CO_2^-Na^+)_2$. The key feature (as discussed above) is the molecular complexity of the salt contents and with no disordered components in the structure.

The asymmetric unit can also be interpreted as comprising four 1,1′-Fc(4-$C_6H_4CO_2^-Na^+)_2$ basic units for dianions *A*–*D* and linked by dianion *E*, two Na^+ ions and three water molecules stabilizing the dianion *E* deformation, with asymmetric units linked by an O—H···O hydrogen-bonded one-dimensional chain (Figs. 3 and 5). This $[Na^+]_{10}$[1,1′-Fc(4-$C_6H_4CO_2^-)_2]_5\cdot3H_2O$ structure has to significantly offset the energy cost of the deformation of the pendant groups in dianions *E* and *C* from parallel. This energy cost is offset by the large number of ionic bonds formed in the central ionic core of each asymmetric unit and involving a combination of Na^+···{O^-, O), H_2O} ionic bonds extending through the lattice as two-dimensional sheets. Overall packing comprises the two-dimensional layers of Na^+ ions coordinated mainly by the carboxylate O atoms, and one-dimensional zigzag chains of water molecules: the non-polar $Fc(C_6H_4)_2$ groups are arranged perpendicular to these layers and mutually interlock through a series of efficient C—H···π stacking contacts in a herringbone fashion to produce an overall segregation of polar and non-polar entities in the crystal structure of (II).

It is pertinent to refer to structures with high Z' numbers. Two examples include:

(i) the fluorinated amphiphile 1-(perfluorobutyl)undecanoic acid $CF_3(CF_2)_3(CH_2)_{10}COOH$ (Z' = 5; Lehmler *et al.*, 2004), with the high Z' ascribed to 'the conflict between the necessity of filling space densely and uniformly and the tendency of unlike groups to be segregated spatially' and

(ii) *N*′′-cyano-*N*,*N*-diisopropylguanidine (Z' = 10), where molecular pairs associate to form ribbons that twist into a helix having five dimers per turn (Hao *et al.*, 2005).

Every high Z' crystal structure has its own particular intricate attributes resulting from both molecular and aggregation level characteristics. These crystal structures necessitate examination in detail separately and also for highlighting comparisons with closely related low Z' structures. Such is the case for (II) which can be classed as an unusual Z' = 5 complex salt comprising both ionic (polar) components and non-polar components that are spatially segregated.

4. Related ferrocene literature

Although there are no comparable 1,1′-Fc[($C_6H_4CO_2^- M^+$)$_2$] salts, a related series of pyridine compounds, 1,1′-Fc[(C_5NH_4)$_2$] have been described (Braga, Polito *et al.*, 2003; Braga *et al.*, 2008). Distortions in the pyridine angles are typically < 10° in the *cisoid* structures with the C_5H_4 and pyridine rings essentially parallel and the pyridine rings mutually parallel (on steric grounds). The few cases where either of these angles are 10–20° have small ring rotations along the C_{ipso}—N axis and accommodated by rotations from the idealized C_5 eclipsed geometries by $n \times 72°$ (n = 1 or 2) from an ideal 0°. Perturbations (or opening) of the two C_5H_4—C_5NH_4 (cp-py) groups are small and typically < 5°.

Of interest is GUVLUE, a heterometallic salt (Kondo *et al.*, 2003) which contains six 1,1′-Fc(CO_2)$_2$ dianions bonded to a tridecamanganese cationic core *via* carboxylates and with bridging methoxy/oxo groups assisting in stabilizing the structure. The Fc groups are oriented in an octahedral fashion from the Mn13 core (comprising Mn4/Mn5/Mn4 units): it is described as a nanoscale ferrocene assembly supported by a supercubane framework. There are no comparable structures analogous to (II) or GUVLUE and it is unlikely (though not impossible) that the smaller 1,1′-Fc(CO_2)$_2$ dianions in GUVLUE would have the flexibility to bend to accommodate distortions such as in (II).

5. Group bending in organometallic and inorganic complexes

Bending in compounds containing rigid ferrocene groups/chains is energy demanding in contrast to ring rotation about C—C axes at the C_{cp}—C_{ar} and/or the C_{ar}—$C_{carboxylate}$ linkages. Thus, bending along chains of aromatic groups comprising —(C_6H_4)$_n$— is rare and distortions are usually accommodated by ring twisting around the central $C_{ipso/para}$ axis than through bending along the entire chain. Examples include 1,1′-bis(5-(4′′-*N*,*N*-diphenylamino-1,1′:4′,1′′-terphenyl-4-yl)-1,3,4-ferrocene) toluene solvate (CIXFEV) where both twisting and minor bending occurs (Chiang *et al.*, 2008) and 4-nitro-4′′-ferrocenyl-1,1′:4′,1′′-terphenyl (YAYRAS) where the terphenyl group is relatively unperturbed (Makarov *et al.*, 2004).

By contrast, deformation of poly(yne) chains are well documented, *e.g.* μ_2-dodecahexayne-1,12-diyl-tetracarbonyl-bis(η^5-pentamethylcyclopentadienyl)diiron (LAQBOU; Sakurai *et al.*, 1999) and nitrosyl-(η^5-pentamethylcyclopentadienyl)(triphenylphosphine)-(8-4-tolyl-1,3,5,7-hexatetrayne)-rhenium (BEJCEY; Dembinski *et al.*, 1999). However, the one-dimensional bending of poly(yne)s contrasts with the distortions in (II) which involve a combination of one-dimensional (C—C linkers) and two-dimensional bending (C_6 rings), although the former predominates in the dianion *E* of (II).

While (II) differs considerably from the metal-organic frameworks frequently encountered in transition metal chemistry (Tranchemontagne *et al.*, 2009), it nonetheless contains features that encompass organometallic, organic, coordination and materials chemistry (Kühnert *et al.*, 2009) as well as hydrogen-bonding studies. The crystal structure of (II) may stimulate further studies encompassing these areas with a view to novel structures, spectroscopic and electrochemical applications.

6. Conclusions

We view the formation of (II) as [Na^+]$_2$[1,1-Fc(4-$C_6H_4CO_2^-$)$_2$]·0.6H_2O with Z' = 5 as fortuitous and best understand that it has arisen under unusual crystallization conditions. Further research on (I), (II) and related systems is planned by varying the alkali metal cation starting materials and solvent crystallization conditions in order to probe the variety of possible compounds and structures that can be isolated, analysed and structurally characterized. Our inability to crystallize a simple salt despite repeated attempts using over 100 solvent conditions is both peculiar and interesting. Despite the low yield in the synthesis of (I), efforts are on-going to improve the synthetic yield and applicability of these and related 1,1′-Fc-based dicarboxylates.

JFG thanks Dublin City University for grants in aid of undergraduate research and the National Institute of Cellular Biotechnology, DCU for research funding under the Irish Government PRTLI #3 funding round (2001–2008).

References

Allen, F. H. (2002). *Acta Cryst.* B**58**, 380–388.
Anderson, F. P., Gallagher, J. F., Kenny, P. T. M., Ryan, C. & Savage, D. (2003). *Acta Cryst.* C**59**, *m*13–*m*15.
Bera, J. K., Clerac, R., Fanwick, P. E. & Walton, R. A. (2002). *J. Chem. Soc. Dalton Trans.* pp. 2168–2172.
Blessing, R. H. (1995). *Acta Cryst.* A**51**, 33–38.
Braga, D., Giaffreda, S. L., Grepioni, F., Palladino, G. & Polito, M. (2008). *New J. Chem.* **32**, 820–828.
Braga, D., Maini, L., Grepioni, F., De Cian, A., Felix, O., Fischer, J. & Hosseini, M. W. (2000). *New J. Chem.* **24**, 547–553.
Braga, D., Maini, L., Polito, M., Mirolo, L. & Grepioni, F. (2003). *Chem. Eur. J.* **9**, 4362–4370.
Braga, D., Polito, M., Bracaccini, M., D'Addario, D., Tagliavini, E., Sturba, L. & Grepioni, F. (2003). *Organometallics*, **22**, 2142–2150.
Butler, I. R., Hobson, L. J., Coles, S. J., Hursthouse, M. B. & Malik, K. M. A. (1997). *J. Organomet. Chem.* **540**, 27–40.
Chiang, C. C., Chen, H.-C., Lee, C.-S., Leung, M.-K., Lin, K.-R. & Hsieh, K.-H. (2008). *Chem. Mater.* **20**, 540–552.
Cotton, F. A., Daniels, L. M., Lin, C. & Murillo, C. A. (1999). *J. Am. Chem. Soc.* **121**, 4538–4539.
Deck, P. A., Lane, M. J., Montgomery, J. L., Slebodnick, C. & Fronczek, F. R. (2000). *Organometallics*, **19**, 1013–1024.
Dembinski, R., Lis, T., Szafert, S., Mayne, C. L., Bartik, T. & Gladysz, J. A. (1999). *J. Organomet. Chem.* **578**, 229–246.
Evans, W. J., Sollberger, M. S. & Ziller, J. W. (1993). *J. Am. Chem. Soc.* **115**, 4120–4127.
Ferguson, G. (1998). *PREP*8. University of Guelph, Canada.
Hao, X., Chen, J., Cammers, A., Parkin, S. & Brock, C. P. (2005). *Acta Cryst.* B**61**, 218–226.
Kondo, M., Shinagawa, R., Miyazawa, M., Kabir, M. K., Irie, Y., Horiba, T., Naito, T., Maeda, K., Utsono, S. & Uchida, F. (2003). *Dalton Trans.* pp. 515–516.

Kühnert, J., Rüffer, T., Ecorchard, P., Brauer, B., Lan, Y., Powell, A. & Lang, H. (2009). *Dalton Trans.* pp. 4499–4508.
Lehmler, H.-J., Parkin, S. & Brock, C. P. (2004). *Acta Cryst.* B**60**, 325–332.
Makarov, M. V., Dyadchenko, V. P. & Antipin, M. Yu. (2004). *Russ. Chem. Bull.* **53**, 2768–2773.
Masello, A., Murugesu, M., Abboud, K. A. & Christou, G. (2007). *Polyhedron*, **26**, 2276–2280.
McArdle, P. (1995). *J. Appl. Cryst.* **28**, 65.
Moers, O., Blaschette, A. & Jones, P. G. (2000). *Z. Anorg. Allg. Chem.* **626**, 2409–2418.
Moers, O., Blaschette, A. & Jones, P. G. (2001*a*). *Z. Anorg. Allg. Chem.* **627**, 254–260.
Moers, O., Blaschette, A. & Jones, P. G. (2001*b*). *Z. Anorg. Allg. Chem.* **627**, 95–102.
Nonius (1997). *KappaCCD* Server Software, Windows 3.11 Version. Nonius BV, Delft, The Netherlands.
Otwinowski, Z. & Minor, W. (1997). *Methods in Enzymology*, Vol. 276, *Macromolecular Crystallography*, Part A, edited by C. W. Carter Jr & R. M. Sweet, pp. 307–326. New York: Academic Press.
Sakurai, A., Akita, M. & Moro-oka, Y. (1999). *Organometallics*, **18**, 3241–3244.
Savage, D., Gallagher, J. F., Ida, Y. & Kenny, P. T. M. (2002). *Inorg. Chem. Commun.* **5**, 1034–1040.
Sheldrick, G. M. (2008). *Acta Cryst.* A**64**, 112–122.
Spek, A. L. (2009). *Acta Cryst.* D**65**, 148–155.
Štěpnička, P. (2008). *Ferrocenes.* New York: Wiley Interscience, John Wiley and Sons Ltd.
Štěpnička, P., Zábranský, M., Císařová, I. & Lamač, M. (2008). *J. Organomet. Chem.* **693**, 3831–3841.
Tranchemontagne, D. J., Mendoza-Cortéz, J. L., O'Keeffe, M. & Yaghi, O. M. (2009). *Chem. Soc. Rev.* **38**, 1257–1283.
Vogel, A. I., Furniss, B. S., Hannaford, A. J., Smith, P. W. G. & Tatchell, A. R. (1996). *Vogel's Textbook of Practical Organic Chemistry*, 5th Ed. New Jersey: Prentice Hall.
Yang, Y.-Y. & Wong, W.-T. (2002). *Chem. Commun.* pp. 2716–2717.
Zakaria, C. M., Ferguson, G., Lough, A. J. & Glidewell, C. (2002). *Acta Cryst.* B**58**, 786–802.
Zakaria, C. M., Ferguson, G., Lough, A. J. & Glidewell, C. (2003). *Acta Cryst.* C**59**, m271–m274.